SECOND EUROPEAN CONFERENCE ON EARTHQUAKE ENGINEERING
AND SEISMOLOGY, ISTANBUL AUG. 25-29, 2014

BI-DIRECTIONAL EXPERIMENTAL RESPONSE OF FULL SCALE DCSS DEVICES

Marco FURINGHETTI[1], Chiara CASAROTTI[2] and Alberto PAVESE[3]

ABSTRACT

In last years it has been observed that the lateral response of Concave Surface Sliders (CSS) under bi-directional earthquake excitations may be significantly different in comparison to the uni-directional case. This is mainly due to the stepwise variation of the direction of the frictional force, which is parallel to the device trajectory and no longer parallel to the always radial recentering force: the vectorial sum of this two components of the response results in lower forces along both directions with respect to the uni-directional motion, and in highly non-linear hysteretic loops, which cannot be approximated with the typical bi-linearized standard constitutive law.

The present endeavour shows the results of a wide experimental campaign on a CSS device, performed following a special testing protocol with both uni-directional and bi-directional dynamic tests: the former ones have been used to investigate the tribological characteristics of the device and to calibrate the friction coefficient properties of an analytical model, whereas the latter ones allowed to deeply investigate the main features of the spatial response of the device. Results have shown that all the effects of bi-axial interaction between two simultaneous directions of motion cannot be neglected when designing a structural system, seismically isolated with such a kind of devices.

INTRODUCTION

Most of the experimental and analytic studies on single and double concave surface sliders (SCSS and DCSS, respectively), are focused on uniaxial response (Fenz and Constantinou, 2006). Concerning the bi-directional motion, a limited number of numerical studies are available, and even though experimental tests on full scale devices have been carried out in the past (Becker and Mahin, 2012) the accessible data are limited. Recently, Lomiento et al. (2013) investigated the bi-directional response of a full scale CSS device, subjected to bi-directional orbits with different levels of vertical load. Results of such and previous efforts highlighted four main characteristics of the sliding material employed within CSS devices: i. the breakaway effect, responsible for the sudden force increase at the beginning and at each motion reversal (stick-slip); ii. the reduction of the friction coefficient at high values of applied vertical pressures; iii. the variation of the friction coefficient with respect to the sliding velocity; iv. and the cycling effect, that is the decay of the friction coefficient during dynamic tests due to the heating originated at the sliding interfaces.

A recent numerical research on a system isolated with CSS devices (Furinghetti et al., 2012) has been carried out using a bi-directional model of the DCSS where mounting laying defects have been considered in the global response. In that endeavour, the implementation of an improved mechanical model of the device is presented, calibrated on the outcomes of several experimental campaigns

---

[1] Ph.D. candidate, UME School, Pavia (Italy), marco.furinghetti@umeschool.it
[2] Ph.D, EUCENTRE, Pavia (Italy), chiara.casarotti@eucentre.it
[3] Associate Professor, University of Pavia, Pavia (Italy), a.pavese@unipv.it

performed at TREESLab Bearing Tester System at Eucentre Foundation (Pavia, Italy). Such a research work has shown analytically that the bi-directional lateral response of a CSS device is significantly different in comparison to the uni-directional one, implying thus that this aspect cannot be neglected in the design/modeling phase of a seismically isolated structure.

In the present document the bi-directional response of a DCSS device is investigated, presenting the results of an experimental campaign carried out by means of the new testing setup for tri-axial tests implemented at the EUCENTRE TREES Lab. Ad hoc testing protocol has been defined, considering both uni-directional and bi-directional tests, in order to fully characterize the friction properties and the biaxial response of the device: 1D tests have been used to calibrate the frictional characteristics of the device, according to the common practice. Then, a number of bi-directional orbits have been performed. For both 1D and 2D tests, special custom input signals have been defined, generated with a special resampling procedure, able to return input signals with stepwise constant modulus of the tangent velocity, in order to eliminate the influence of the velocity variation on the friction coefficient, and to isolate and stabilize the friction properties for each given test.

Common standard orbits have been as well performed, in order to evaluate the differences of considering a constant rather than a fluctuating modulus of the velocity during the motion. At the end of the testing protocol, an earthquake simulation has been run, with an input signal obtained by means of the time-integration of the equation of motion of a single oscillator, isolated with a bi-directional DCSS devices by using the aforementioned model (Furinghetti et al., 2012). Due to the large number of performed tests, the device wear has been monitored during the whole test campaign by means of repeated benchmark tests.

TRI-DIMENSIONAL TESTING SETUP

A special testing setup has been installed at the EUCENTRE TREES Lab in Pavia, in order to carry out tri-dimensional tests. The Bearing Tester System shown in Fig.1 (left) has been specifically designed to carry out static and dynamic tests on isolation and dissipation devices. The base table (1.7 m x 4.3 m) allows vertical, longitudinal, roll, pitch and yaw degrees of freedom, under a static vertical load up to 40000 kN and an additional dynamic vertical load up to 10000 kN, whereas the maximum allowance of longitudinal force is 2828 kN. The maximum longitudinal stroke is +/-450mm, with a peak velocity of 2.2 m/s. The BTS Controller is an MTS real-time, digital controller that provides PID closed loop control with a delta-p feedback signal.

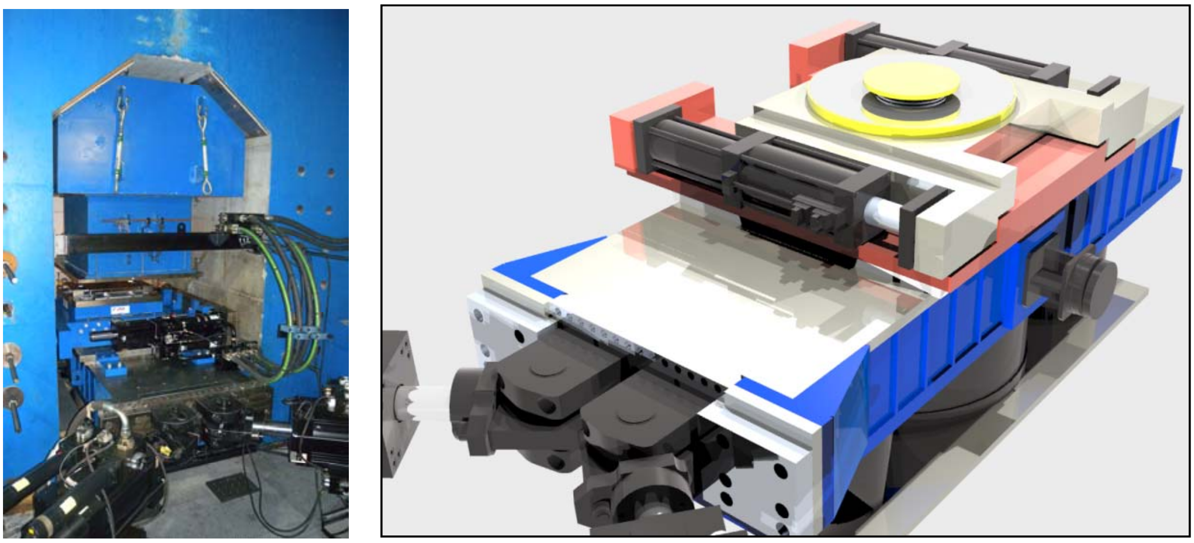

Figure 1. Bearing Tester System: original layout (left) and 3D setup (right)

For tri-dimensional tests a new sliding bench has been implemented within the original system, which allows the transverse translational degree of freedom (Fig.1 right). With such a configuration, bi-directional orbits and earthquake simulations can be performed. For the transverse degree of freedom, a total stroke of +/-260mm and a peak velocity of 0.6m/s can be reached, with a horizontal force capacity equal to 1000kN.

The force feedback response is generally measured by the load cells at the connection between the actuators and the respective bench. Thus, the recorded data contain the force of the device together with the summation of the frictional and inertial forces originated by the testing machine: these two contributions have to be removed in the data reduction phase, in order to consider the solely device force. For this scope, an innovative recording system has been designed ad hoc, aiming at capturing only the force response of the device, without any interference coming from the testing machine. The system consists of a steel plate, 80mm thick, laid on a rubber sheet: such a steel plate is connected to the testing machine by means of eight load cells, as shown in Fig.2.

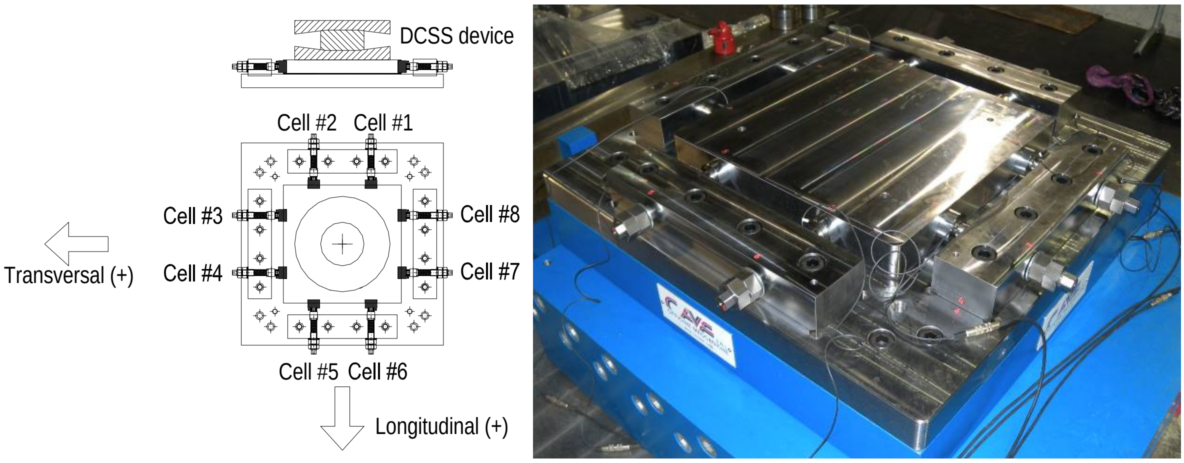

Figure 2. Force Recording rig

All the load cells have been pre-loaded with a compressional force of about 150kN. The total force response has been obtained from the vectorial summation of the load cells measurements, removing the initial offset of the force time history. On the other hand, the displacements recordings are returned by the control software of the testing system, whereas both the velocity and acceleration responses are computed by means of direct time-derivation of the displacement signals.

TESTING PROTOCOL

The device consists of a Double Concave Sliding Surface bearing, having an equivalent radius of curvature equal to 3.1m: both the upper and lower sliding surfaces have a radius of curvature R_{eq} equal to 1.6m and the non-articulated slider has a horizontal diameter of 260mm and a vertical height of 100mm.

A special testing protocol has been defined, with both uni-directional and bi-directional tests for a comprehensive characterization of the lateral response of the device. In both cases entrance and exit loops have been implemented to guarantee the “zero initial condition” (zero displacement and acceleration and given velocity) at the beginning of the first loop and at the end of the last loop.

According to the common practice and to the standard code regulations (e.g. AASTHO , 2010 or CEN, 2009), the input signal for uni-directional tests is a sinusoidal waveform, with periodically varying velocity. The ideal input signal for frictional characterization would be a triangular waveform, because of its constant velocity: however, at high speed, the instantaneously change in the velocity sign at the cycle inversion may jeopardise the testing system stability. The input signal studied for the test presented in the present paper features a combination of triangular and sinusoidal waveform, able to keep the maximum velocity over a wide range of displacement.

For bi-directional tests, a number of bi-directional and stepwise linear orbits have been studied, with maximum radial displacement D_{max} of 0.2m, and with a maximum value of tangent velocity of 0.356m/s, obtained from the sliding frequency of the device.

Stepwise linear orbits (box and hourglass, Fig.3 – Mosqueda et al., 2004) show the behaviour of a CSS device subjected to linear trajectories featuring the following characteristics: i. constant offsets in the direction orthogonal to the motion for part of the orbit, which means corresponding constant value of the recentering force, ii. sudden and sharp direction changes, which imply stick slip effect, and iii. radial motion for part of the hourglass orbit. The overall lateral response for both the planar directions is expected to be stepwise linear as well as in the uni-directional case, with lower values of the "apparent" friction coefficient when the motion is radial, since the friction force is decomposed in the two main directions. Over each of the linear branches of such orbits, a wide range with constant velocity has been implemented.

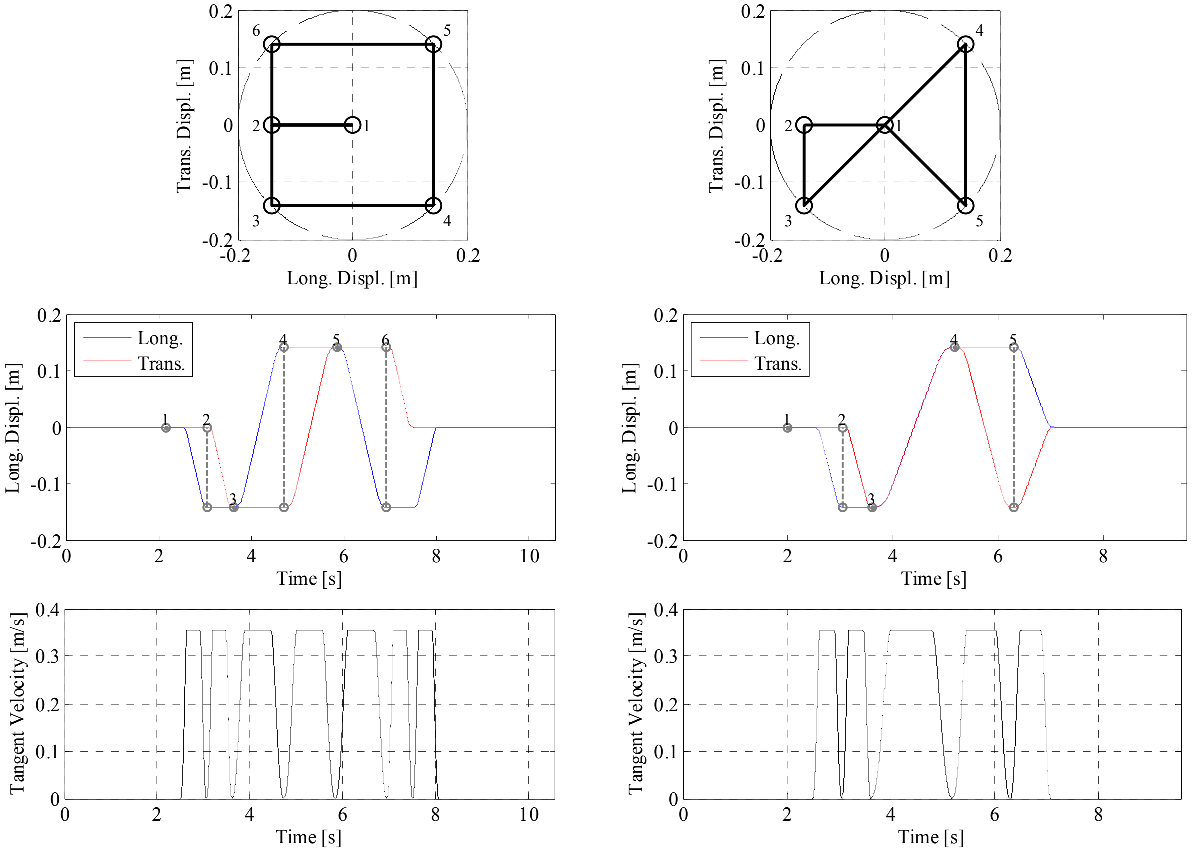

Figure 3. Bi-directional stepwise linear orbits

Then, cloverleaf, eight-shape, spiral and circular orbits have been implemented (Fig.4). A special re-sampling procedure has been studied, aiming at obtaining bi-directional orbits with a stepwise constant value of the tangent velocity modulus. Such curvilinear orbits can be used for a detailed analysis of the force components interaction occurring under bi-axial motion: a comparison of the results of these particular orbits with the application of the single uni-directional components is done, in order to show the differences of accounting for a bi-directional rather than a uni-directional behaviour for a given displacement time-history. Additionally, the cycling effect due to the sliding interfaces heating can be evaluated and compared to the results of uni-directional tests.

Table 1 shows the list of the main characteristics of uni-directional tests, i.e. maximum displacement and velocity, vertical load and number of cycles: basically, the characterization has been conducted on 4 levels of vertical load W, for 9 velocity intensities V. Two full cycles per test have been run (plus entrance and exit loops), in order to limit the wear of the sliding material under such a demanding testing protocol. The WEAR CHECK test is a benchmark test at the beginning, during and at the end of the whole testing protocol, in order to monitor the level of the sliding material wear and to consequently detect possible changes in the frictional properties of the device due to the wear. The results of uni-directional tests have been used to characterize the frictional behaviour with respect to both sliding velocity and vertical load.

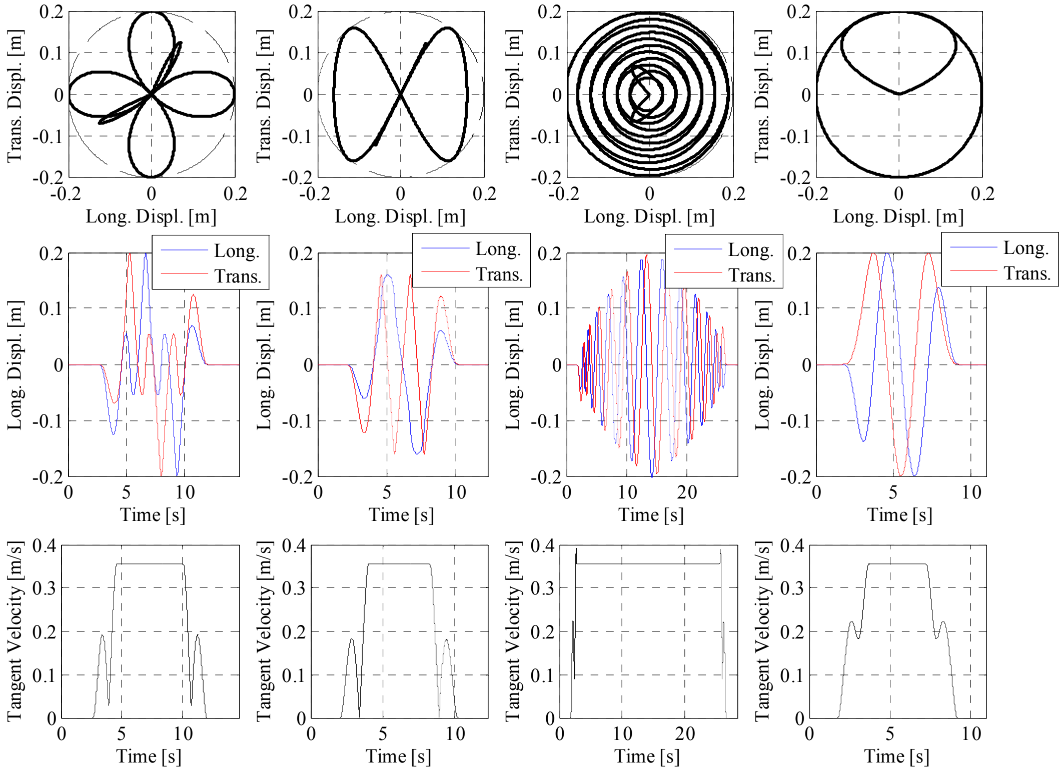

Figure 4. Bi-directional curvilinear orbits

Table 1. Uni-directional testing protocol

Test #	Test Name	Max Displacement [m]	Max Velocity [m/s] V	Vertical Load W [kN]	Cycles [#]
1	WEAR CHECK	±0.200	0.356	2000	2
2 to 10	1D - friction calibration	±0.200	0.015 0.030 0.050 0.065 0.080 0.100 0.200 0.356 0.500	1000	2
11 to 19	1D - friction calibration	±0.200	0.015 0.030 0.050 0.065 0.080 0.100 0.200 0.356 0.500	1300	2
20 to 28	1D - friction calibration	±0.200	0.015 0.030 0.050 0.065 0.080 0.100 0.200 0.356 0.500	1600	2
29 to 37	1D - friction calibration	±0.200	0.015 0.030 0.050 0.065 0.080 0.100 0.200 0.356 0.500	2000	2
38	WEAR CHECK	±0.200	0.356	2000	2

In Table 2 the bi-directional testing protocol is listed. The bi-directional protocol consists of: i. two stepwise linear orbits; ii. cloverleaf and 8-shape orbits, performed both with Constant Tangent Velocity (CTV) and with the ordinary signals (xy); iii. uni-directional components x and y of the latter orbits, in order to show the bi-axial interaction of the frictional forces and the differences between a bi-axial motion and a purely radial motion with the same component; iv. spiral and circle orbits, with CTV; v. earthquake simulation.

To get the input signals for the earthquake simulation, the equations of motion of a single oscillator with the mechanical model of the analysed device has been directly integrated: the numerical model assumes a lumped mass above the isolation level, and considers only the translational degrees of freedom. For such a simulation the 1994 Northridge earthquake has been used, scaling both the records by the same factor, in order to control both the maximum radial displacement and the maximum tangent velocity. Fig.5 shows the displacement response.

The last test is a longer wear check (8 cycles), used to study the frictional response under a large number of cycles. The test has been used to define a new simple formulation for the cycling effect.

Table 2. Bi-directional testing protocol

Test #	Test Name	Max Displacement [m]	Max Velocity V [m/s]	Vertical Load W [kN]	Cycles [#]
38	2D - box orbit	±0.200	0.356	2000	-
39	2D - hourglass orbit	±0.200	0.356	2000	-
40	2D - cloverleaf orbit - CTV	±0.200	0.356	2000	-
41	2D - cloverleaf orbit - xy	±0.200	0.356	2000	-
42	2D - cloverleaf orbit - x	±0.200	0.356	2000	-
43	2D - cloverleaf orbit - y	±0.200	0.356	2000	-
44	2D - 8-shape orbit - CTV	±0.200	0.356	2000	-
45	2D - 8-shape orbit - xy	±0.200	0.356	2000	-
46	2D - 8-shape orbit - x	±0.200	0.356	2000	-
47	2D - 8-shape orbit - y	±0.200	0.356	2000	-
48	2D - Spiral orbit - CTV	±0.200	0.356	2000	-
49	2D - Circle orbit - CTV	±0.200	0.356	2000	-
50	WEAR CHECK	±0.200	0.356	2000	2
51	2D - Earthquake response - 75% W	-	-	1500	-
52	WEAR CHECK - FINAL	±0.200	0.356	2000	7

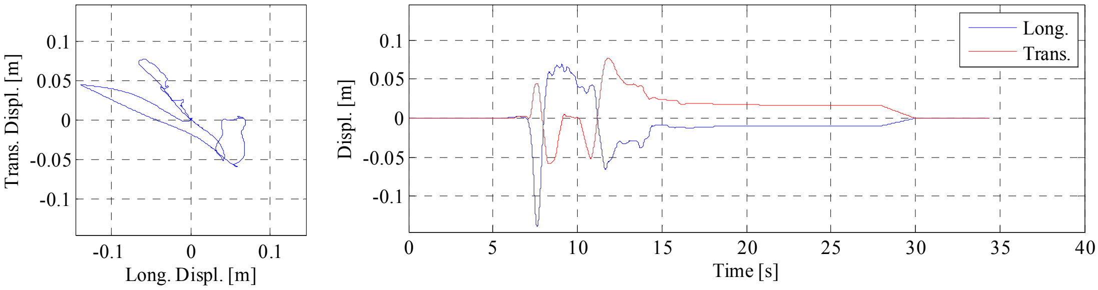

Figure 5. Bi-directional earthquake simulation

EXPERIMENTAL RESULTS

The wear test run throughouth the full testing campaign has demonstrated that the sliding material has not encountered significant degradation, so the test results presented in what follows has not been importantly affected by the wear.

Unidirectional tests

The uni-directional tests have been used to characterize the frictional characteristics of the device as a function of sliding velocity and vertical load. It has to be noted that the device is a double sliding surface device, having two curved surfaced with the same curvature radius, which means that the average effective velocity at the sliding interfaces is half of the applied device velocity. Moreover, the dependence on the vertical load is actually on the applied pressure, i.e. a function also of the slider size.

The dynamic friction coefficient value of the first hysteretic cycle has been computed, according to the standards CEN (2009)(par. 8.3.4.1.5, Eq. 30) as a function of the dissipated energy, thus a friction coefficient value averaged over the cycle.

Hence, all the friction coefficient values have been plotted with respect to both the sliding velocity and the vertical load (Fig.6). As expected, results show the typical behaviour of the friction coefficient with respect to both sliding velocity and vertical load (Contantinou et al, 1990; Lomiento et al., 2013; Casarotti et al. 2013). With respect to sliding velocity (Fig.6 left), the trend of the curves looks very similar for all the levels of vertical loads, showing higher values of friction coefficient as the sliding velocity increases. Furthermore, it is noted that also the lower bound for the friction coefficient (at low velocities) depends on the vertical load (Khoshnoudian1 and Hagdoust, 2009). Fig.6 (right) shows that for all the velocity levels the friction coefficient decreases as the vertical load increases (Contantinou et al, 1990): all the curves fall within a small range of variation (less than 0.02, on stable asymptotic values), which underlines the limited velocity effect with respect to the vertical load effect (> 0.45, not stable).

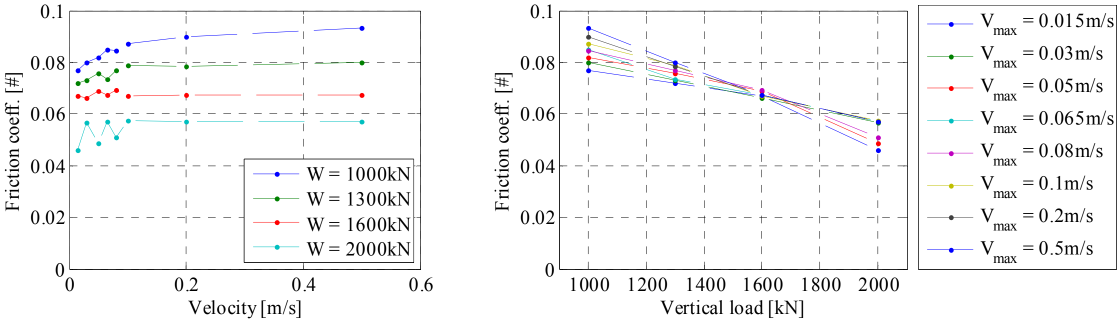

Figure 6. Dependence of the friction coefficient on the sliding velocity (left) and vertical load (right)

Bidirectional Tests

The bi-directional tests are analysed in terms of hysteretic loops and time histories of the force response along both longitudinal and transverse directions.

Results of the stepwise linear bi-directional orbits are shown in Fig.7. It is possible to observe that also the force response can be stepwise linearized, when the trajectory of the device is made up of linear branches. A significant increasing of the lateral force can be detected along the transverse response of the hourglass orbit when the maximum and minimum displacements are reached, mainly due to the sudden changing of direction of the device. Such a sharp direction change can cause rotations of the non-articulated slider, which in turn may lead to unexpected values of lateral force. This aspect has been also noted in uni-directional tests, during which transvers forces have been measured, with peak values up to 16% of the maximum longitudinal force: the rotation of the slider has been experimentally observed during high speed tests.

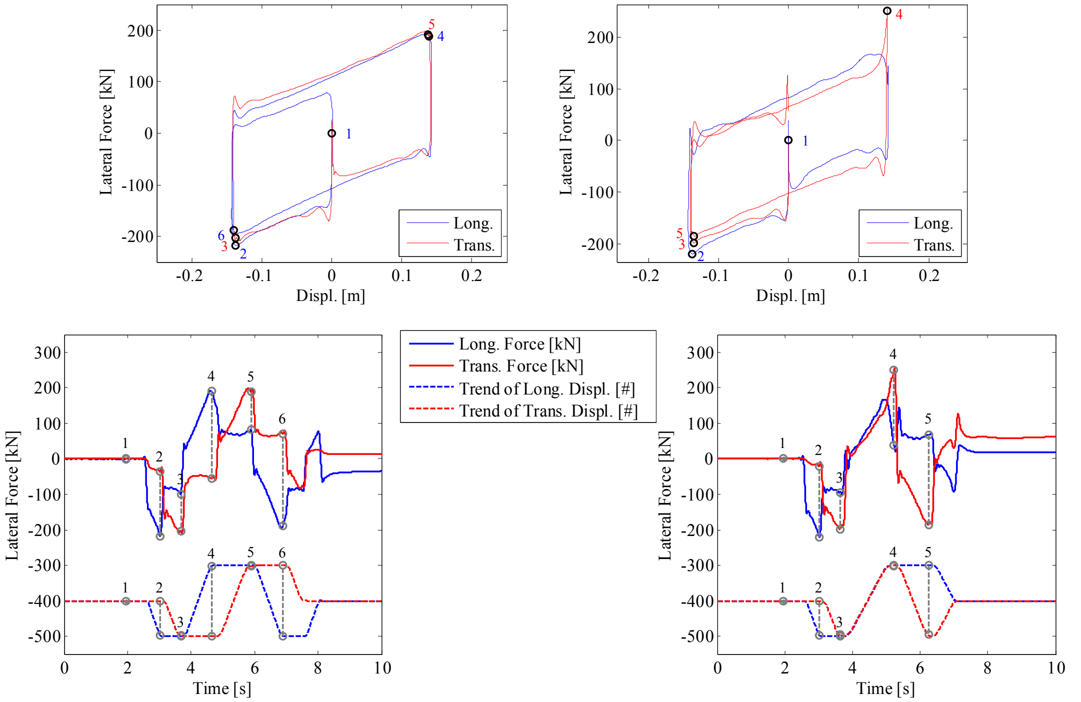

Figure 7. Hysteretic response of stepwise linear bi-directional orbits: box (left) and hourglass (right) orbits

In what follows, results of the curvilinear orbit tests are illustrated. The cloverleaf and 8-shape orbits are shown in Fig.8 and Fig.9, respectively. It can be noted that the bi-axial motion leads to highly non-linear hysteretic loops, very different from the theoretical loop, but also from the regular loops obtained in the tests where the longitudinal and transversal components of the orbits have been separately applied to the device ("uni-directional" component, green line in the figures). The bi-axial motion leads to lower peak forces along both directions: this effect is due to the variation of direction of the frictional force, when both the components are applied simultaneously: the total frictional force is no longer parallel to the restoring force (always radial) and they are not simply summed up as during the unidirectional motion. Such a frictional force can be assumed to be applied along the trajectory of the device, if no rotations of the slider occur. Instead in a uni-directional motion, the total frictional force is applied along the unique direction of motion for the whole duration of the test.

Hysteretic loops of CVT and ordinary orbits are almost overlapped for both the cloverleaf and the 8-shape tests, despite the variation of the velocity along the standard orbits. This is due to the fact that the friction coefficient is rather constant after 0.15m/s for all levels of vertical loads (Fig.6): thus, the differences between the two typologies of tests are negligible.

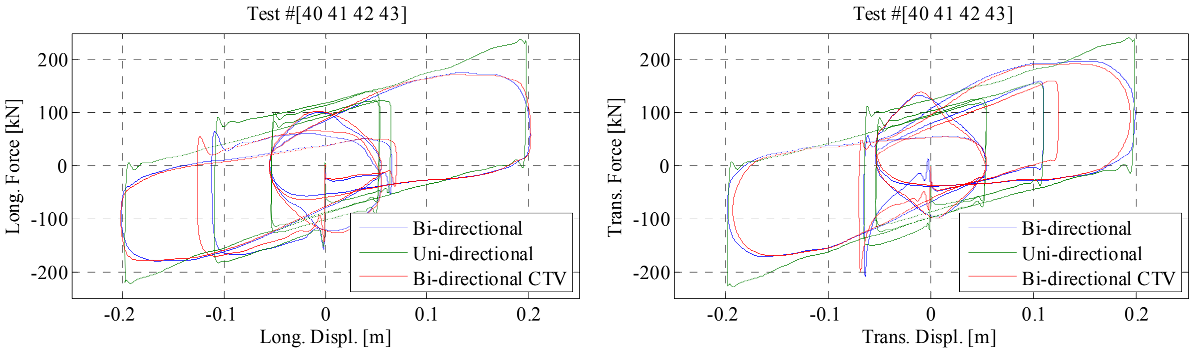

Figure 8. Hysteretic response of cloverleaf orbit: longitudinal (left) and transversal (right)

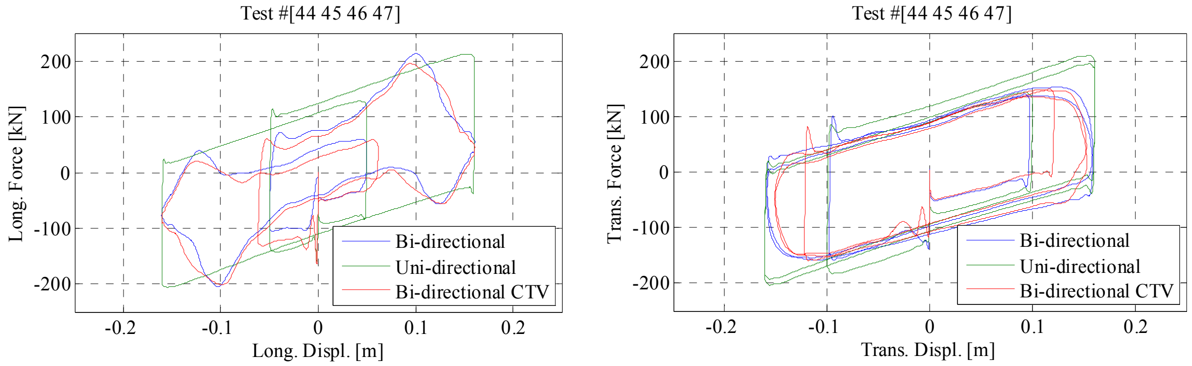

Figure 9. Hysteretic response of 8-shape orbit: longitudinal (left) and transversal (right)

In Fig.10 the results for the spiral and circle orbits are shown. The hysteretic response along both directions is interesting if related to the characteristics of these two particular orbits. The most important feature of the circle orbit is that the restoring force modulus is constant during the test, (being constant the distance from the centre of the device) and always orthogonal to the frictional force. The two constant forces are decomposed and summed up along the main directions according to a sine and a cosine of the same angle: as expected, results show ellipsoidal hysteretic loops along both directions, rotated of an inclination equal to the device recentering stiffness, obtained dividing the vertical load W by the equivalent radius of curvature R_{eq}.

Concerning the spiral motion it is noted that: i. the restoring force increases (due to the gaining displacement), ii. restoring and friction forces are no longer perfectly orthogonal, but they tend to be perpendicular at high displacements. The hysteretic response is similar to that of the circle orbit, consisting in an inclined ellipsoidal loop with increasing area and decreasing thickness.

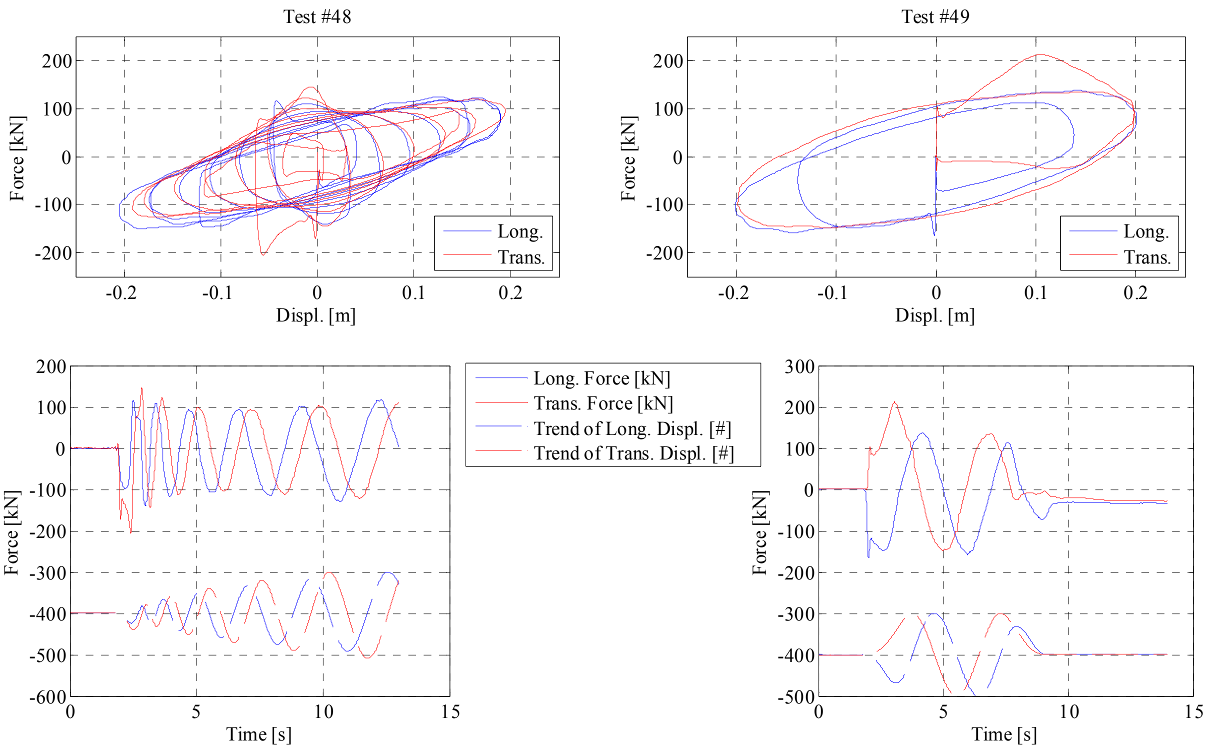

Figure 10. Spiral and circle bi-directional orbits

Friction coefficient decay

The FINAL WEAR CHECK has been used to evaluate the friction coefficient decay after a large number of cycles and calibrate an equation to account for the cycling effect, by means of a non-linear fitting procedure (Eq. (1) and (2)). Since the friction coefficient decay can be attributed to the heating of the sliding surfaces, it has appeared to be natural to search for a correlation with the dissipated energy:

$$\mu_d = k_E \cdot \mu(V,W) \tag{1}$$

$$k_E = a_1 e^{a_2 E} + a_3 \tag{2}$$

where μ_d is the dynamic friction coefficient, μ is the expression which describes the dependency on the sliding velocity V and the vertical load W, k_E represents a decay factor, function of dissipated energy E (integral of the scalar product between the force vector and the differential variation of the displacement vector), and a_1, a_2 and a_3 are the parameters to be calibrated.

Fig.11 shows the cycles of the final wear check tests and the friction coefficient decay rate.

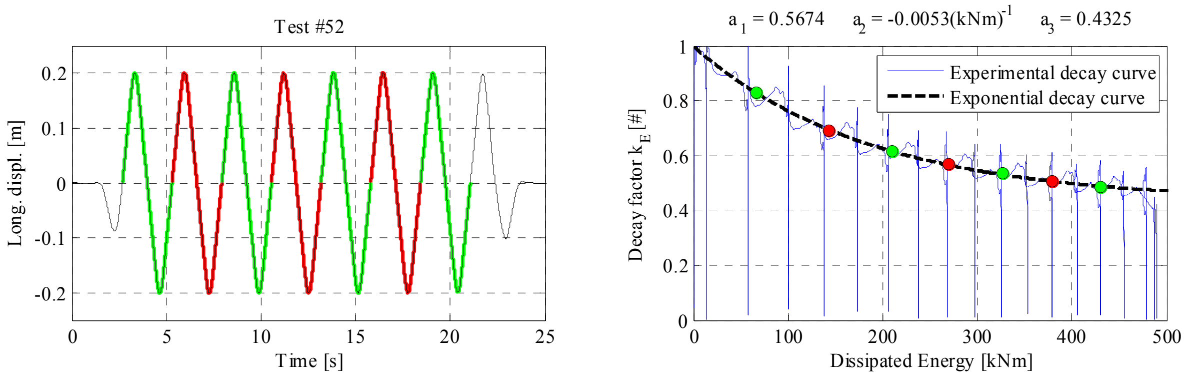

Figure 11. Decay law of the friction coefficient with respect to the dissipated energy

Results of CTV orbits have been used to validate the decay model and to analyse the friction coefficient decay during the biaxial motion. For all the CTV orbits a “tangent” friction coefficient has been calculated as istantaneous value given by the square root of the sum of the squares of the frictional forces along both directions, divided by the vertical load. The attribute “tangent” stands to underline that it related only to the frictional force no longer parallel to any of the main directions of motion.

For all the CTV orbits, the tangent friction coefficient has been plotted with respect to the dissipated energy, together with the uni-directional final wear check tests and the corresponding calibrated decay curve model (Fig.12); for all the bi-directional tests, the range in which the tangent sliding velocity is constant is graphically bounded between the vertical dashed lines.

Fig.12 shows that the decay curve obtained from the uni-directional test is a lower bound for all the experimental decay curves related to the bi-directional orbits: discarding the several fluctuations, the mean bidirectional friction curve follows the same trend of the decay curve calibrated on unidirectional tests, with values averagely larger than 22%. The fluctuations can be due to the oscillations of the vertical load and to the possible rotation of the slider, given that the velocity is fairly constant during the considered tests. It has to be investigated if the bi-axial motion could somehow amplify such effects. The CTV tests have been run at the same peak velocity value (0.356m/s): it has to be investigated if the decay is also function of the velocity, rather than of the cumulative path (Lissia, 2012).

The fact that the friction appears to be larger during bi-axial motion deserves particular attention. This can be attributed to additional internal forces developed at the sliding interfaces due to the rotation of the slider, which has been observed also during unidirectional tests. In fact, even though the uni-directional tests are expected to originate lateral force in the direction of motion only, forces in the transverse direction have been measured, up to 16% of the longitudinal peak force. This aspect may be important and needs further research.

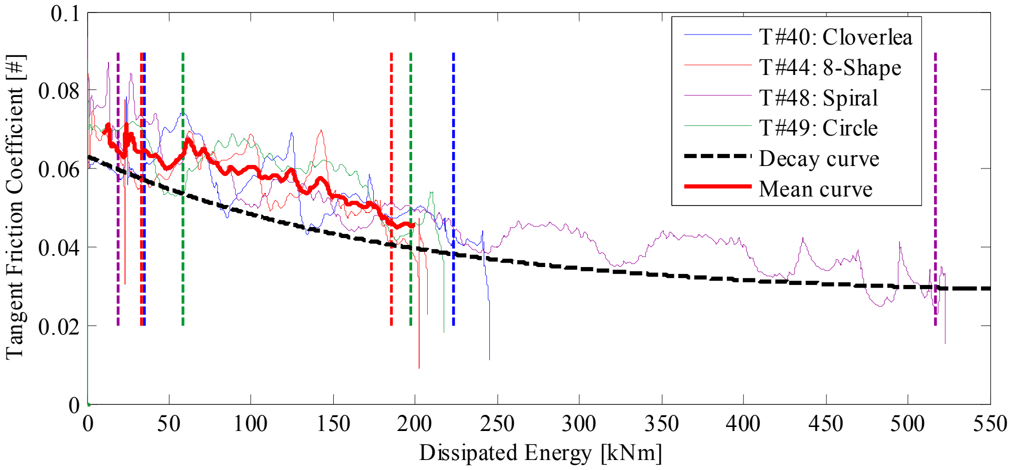

Figure 12. Decay of the tangent friction coefficient with bi-directional orbits

Finally, the results of the earthquake simulation are shown in Fig.13 in terms of hysteretic loops and time histories of horizontal force along both the motion directions. In the same figure, analytical results are plotted, obtained from the bi-directional model defined by Furinghetti et al. (2012). A constant friction coefficient equal to 7% has been used, corresponding to an average value obtained from Fig.6 corresponding to the applied vertical load.

As expected, it is noted that during a bi-directional earthquake excitation, the response of a CSS device cannot be modelled with a bi-linear hysteretic loop, by simply decoupling the motion along the two main directions, since it is more complex and strongly coupled. Both the force signals are extremely irregular, mainly due to the continuous variation of the frictional force direction tangent to the motion trajectory. This effect is supposed to be even amplified in case of important fluctuation of the vertical load, especially with high frequency content motions.

The comparison with the analytically computed force response is shown. Even though the friction coefficient has been assumed constant, the model provides a fairly good estimate of the force response of the device.

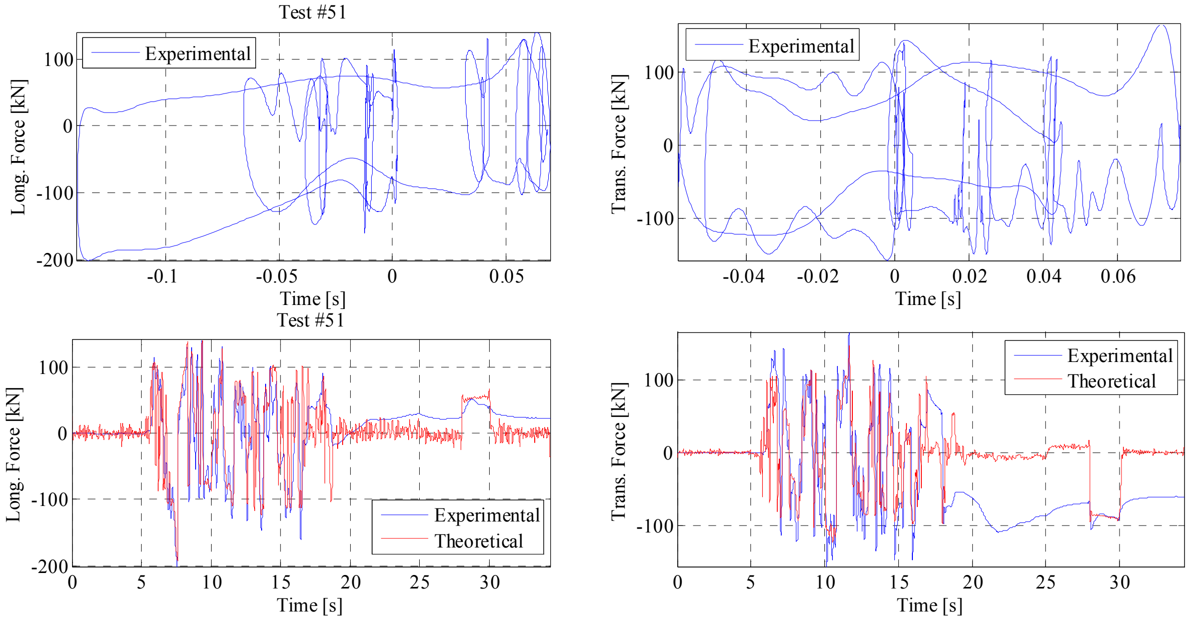
Test #51

Test #51

Figure 13. Earthquake simulation results

CONCLUDING REMARKS AND FUTURE DEVELOPMENTS

In the present endeavour the bi-directional response of a CSS device has been investigated by means of an intensive experimental campaign. A special testing protocol has been studied focused to the careful and accurate definition of the tribological properties of the sliding material. Attention has been concentrated on the dependency of the dynamic friction coefficient on the sliding velocity and the vertical load. Firstly, the unidirectional response has been investigated, then, a number of bi-directional tests have been performed, considering standard orbits found in literature. The latter test have been run with stepwise constant tangent velocity (CTV) obtained by means of a special resampling procedure, in order to characterize the bi-directional frictional characteristics of the device without the influence of the velocity variation. Additionally, the decay of the friction coefficient due to heating effect has been studied, calibrating a simple analytical formulation.

Results for uni-directional tests show the typical response of a friction-based device with respect to both vertical load and sliding velocity: the higher the vertical load, the lower the friction coefficient; whereas, the friction coefficient increases as the sliding velocity increases. However, it has been found that also the friction coefficient at low velocities depends on the vertical load.

Bi-directional stepwise linear orbits have shown that the lateral response of a CSS device subjected to linear orbits with initial offsets with various radial directions is stepwise linear as well. Curvilinear orbits have been run both as bidirectional motion and as separated unidirectional components: as expected, running the single component leads to higher values of both peak force and dissipated energy, with respect to the bidirectional motion, due to the parallelism of the restoring force and of the friction force in the former case. It has been observed that CTV orbits returned hysteretic loops approximately overlapped to the ones returned by the corresponding ordinary input: this is mainly due the fact that the velocity oscillations of the ordinary signals fall in the range of friction coefficient approximately constant with the velocity.

As already shown by previous analytical studies, physical models and experimental investigations, the performed bi-directional testing campaign made evident that the response of a CSS device cannot be modelled with a bi-linear hysteretic loop, by simply decoupling the motion along the two main directions: the response closest to the standard modelling could be that of mainly unidirectional seismic motion, otherwise it would lead to an important overestimation of the force response along both directions.

The heating effect has been studied by means of a test with a large number of cycles, observing the decay of the friction coefficient. A new formulation of such effect is reported, which expresses the decay as an exponential function of the dissipated energy. The curve represents the heating effect at the design vertical load and velocity. Similar response has been observed during the bidirectional motion, with comparable decay trend but slightly larger value of the tangent friction coefficient, and somehow amplified fluctuations, likely due to the vertical load oscillations, possibly increased by bi-axial motion. Such fluctuations and the apparent increase of the friction coefficient during the bi-axial motion can be attributed to secondary forces induced by the rotation of the slider.

The most evident result of the present work basically consists in the experimental proof that the biaxial motion of CSS devices is complex, and rather different by the standard unidirectional response, which cannot be simply used to represent the spatial response of the device during and actual event. Moreover, additional unexpected forces have been measured during the bi-directional tests, which lead to larger values of the tangent friction coefficient. The source of such forces may be attributed to different phenomena: the rotation of the slider and the sudden change in the device trajectory which may induce stick slip effects at higher frequencies. Both aspects need further experimental and analytical investigation.

REFERENCES

AASHTO – American Association of State Highway and Transportation Officials (1999) “Guide Specifications for Seismic Isolation Design”, 2nd Edition. American Association of State Highway and Transportation Officials, Washington DC

Becker TC and Mahin SA (2012) “Experimental and analytical study of the bi-directional behavior of the triple friction pendulum isolator,” *Earthquake Engineering And Structural Dynamics*, (41): 355-373

CEN – Comité Européen de Normalisation TC 340 (2009) “European Code UNI EN 15129:2009 Anti-seismic devices”, Brussels

Constantinou MC, Mokha A, Reinhorn AM (1990) “Teflon bearings in base isolation II: Modeling", *J Struct Eng, ASCE*, 116(2), pp. 455-474.

Fenz D and Constantinou MC (2006) “Behaviour of the double concave friction pendulum bearing,” *Earthquake Engineering And Structural Dynamics*, (35):1403–1424

Furinghetti M, Casarotti C, Pavese A (2012) “Effects of bi-directional motion on a structural system isolated with DCSS devices with laying defects”, 15th WCEE, World Conference on Earthquake Engineering, Lisbon, Portugal

Khoshnoudian F and Hagdoust VR (2009) “Response of pure-friction sliding structures to three components of earthquake excitation considering variations in the coefficient of friction,” *Scientia Iranica*, 16(6 (transaction a: civil engineering)):429-442

Lissia S (2013) Effects of the response modification factors on the CSS isolators: theoretical background, modeling and experimental validation on full scale devices, M.Sc. Thesis, UME School – Understanding and Managing Extremes, Pavia, Italy

Lomiento G, Bonessio N, Benzoni G (2013) “Friction Model for Sliding Bearings under Seismic Excitation,” *Journal of Earthquake Engineering*, 17:8, 1162-1191, DOI: 10 1080/13632469 2013 814611

Lomiento G, Bonessio N, Benzoni G (2013) “Concave sliding isolator’s performance under multi-directional excitation,” *Ingegneria Sismica*, 30(3):17-32

Mosqueda G, Whittaker AS, Fenves GL (2004), “Characterization and modeling of friction pendulum bearings subjected to multiple components of excitation,” *Journal of Structural Engineering*, march 2004: 433-442

Casarotti C, Furinghetti M, Pavese A (2013) “Evaluation of response of an isolated system based on Double Curved Surface Slider,” Computational method in Earthquake Engineering, Volume 30, pp 397-416